Adaptive Kalman Filtering and Smoothing for Gravitation Tracking in Mobile Systems

Simo Särkkä*
Aalto University, Espoo, Finland
IndoorAtlas Ltd., Helsinki, Finland
Email: *simo.sarkka@aalto.fi

Ville Tolvanen
IndoorAtlas Ltd., Helsinki, Finland

Juho Kannala and Esa Rahtu
University of Oulu, Oulu, Finland
IndoorAtlas Ltd., Oulu, Finland

Abstract—This paper is concerned with inertial-sensor-based tracking of the gravitation direction in mobile devices such as smartphones. Although this tracking problem is a classical one, choosing a good state-space for this problem is not entirely trivial. Even though for many other orientation related tasks a quaternion-based representation tends to work well, for gravitation tracking their use is not always advisable. In this paper we present a convenient linear quaternion-free state-space model for gravitation tracking. We also discuss the efficient implementation of the Kalman filter and smoother for the model. Furthermore, we propose an adaption mechanism for the Kalman filter which is able to filter out shot-noises similarly as has been proposed in context of adaptive and robust Kalman filtering. We compare the proposed approach to other approaches using measurement data collected with a smartphone.

Keywords—*Gravitation tracking; Kalman filtering; Kalman smoothing; Adaptive filtering; Smartphone*

I. INTRODUCTION

The accurate tracking of gravitation direction is an important task in many smartphone-based applications. For example, in pedestrian dead reckoning (PDR) systems [1], magnetic field based positioning systems [2]–[4] as well as in basic functionality of smartphones such as in determining the orientation of the screen. The task of gravitation tracking is a common and well studied task, and it is related to classical inertial navigation technology (e.g., [5], [6]). It is also clear that the Kalman filter [7]–[9]—or more precisely *a* Kalman filter—is a suitable tool for this task. However, it is not that clear from current literature what is the best state-space for the Kalman filter and hence what does the practical algorithm actually look like—obviously, a Kalman filter without a specified state-space model is not a practical algorithm at all.

The aim of this article is to present a convenient linear state-space formulation of the gravitation tracking task, as opposed to non-linear state-space model which results from many quaternion-based approaches for orientation tracking (e.g. [5], [6], [10]–[12]). The advantage of this formulation is that it is computationally light and it allows for exact and light Kalman/Rauch–Tung–Striebel smoother (e.g., [9]) implementation on top of the Kalman filter. We also propose an adaptation mechanism for the Kalman filter which is able to filter out shot-noises in a bit similar manner as has been proposed in context of adaptive and robust Kalman filtering [13], [14]. We also compare the proposed approach to other approaches using measurement data collected with a smartphone.
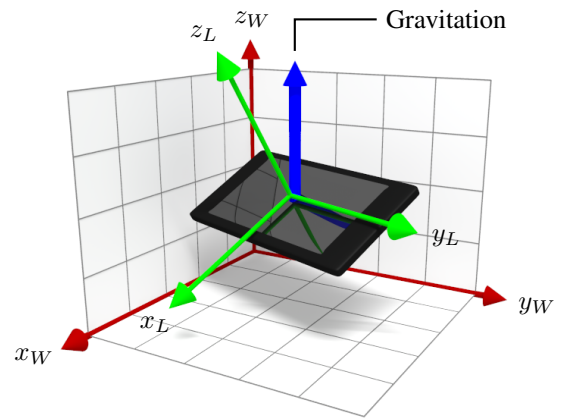

Fig. 1. Illustration of measurement of the gravitation by smartphone accelerometers. Although the measured gravitation acceleration in world (global) coordinates $\mathbf{g}_W$ is constant pointing towards the z_W-direction (i.e., up) in the world coordinate system (x_W, y_W, z_W), the direction of the locally measured gravitation $\mathbf{g}_L$ is depends on the orientation of the local coordinate system (x_L, y_L, z_L) with respect to the world coordinate system. In addition to the gravitation, the acceleration sensors also measure the movement-generated accelerations of the smartphone.

II. QUATERNION-FREE REPRESENTATION OF ORIENTATION

A. How Sensors See Gravitation

Assume that both the acceleration sensor and gyroscope are placed in the same position in the smartphone such that they measure the acceleration and angular velocity in the smartphone-local coordinate system (denoted with subscript L), which is separate from the world coordinate system (denoted with subscript W). The actual measurement returned by the acceration sensor is the sum of the gravitation and the local accelerations as follows:

$$\mathbf{a}_M(t) = \mathbf{g}_L(t) + \mathbf{a}_L(t). \tag{1}$$

We are mainly interested in the gravitation and we believe that it, on average, is the dominant component in the acceleration sensor measurement. Therefore we model the local gravitations as white random perturbations on the gravitation measurement. Thus our basic model assumption is that the acceleration sensor measures the local gravitation plus a Gaussian white noise component $\boldsymbol{\epsilon}(t)$:

$$\mathbf{a}_M(t) = \mathbf{g}_L(t) + \boldsymbol{\epsilon}(t). \tag{2}$$

Although the gravitation in the world coordinate system $\mathbf{g}_W$ is constant, the term $\mathbf{g}_L(t)$ above is not contant, because how gravitation shows in the local coordinate system depends on the device orientation (see Fig. 1). However, at each time t there exists a coordinate transformation $\phi(\cdot, t)$ which converts the world-gravitation into locally measured gravitation:

$$\mathbf{g}_L(t) = \phi(\mathbf{g}_W, t). \tag{3}$$

The coordinate transformation also defines the orientation of the smartphone with respect to the global gravitation.

B. Quaternion Representation

One classical way to define orientation of the device is via a unit quaternion

$$\mathbf{q} = \begin{pmatrix} \cos(\theta/2) \\ \mathbf{u}\,\sin(\theta/2) \end{pmatrix}, \tag{4}$$

which transforms a local vector such $\mathbf{g}_L$ to the corresponding world vector $\mathbf{g}_W$ via the quaternion rotation

$$\mathbf{g}_W = \mathbf{q}\,\mathbf{g}_L\,\mathbf{q}^* \tag{5}$$

that essentially rotates $\mathbf{g}_L$ around vector $\mathbf{u}$ for angle θ. Above products are quaternion products and $()^*$ denotes the quaternion conjugate (see, e.g., [5], [6], [11]). The inverse transformation is given as

$$\mathbf{g}_L = \mathbf{q}^*\,\mathbf{g}_W\,\mathbf{q} \triangleq \phi(\mathbf{g}_W, t). \tag{6}$$

which thus defines the coordinate transformation in (3) where the time-dependence comes from the time-dependence of the quaternion. Thus our model has the form

$$\mathbf{a}_M(t) = \mathbf{q}^*(t)\,\mathbf{g}_W\,\mathbf{q}(t) + \boldsymbol{\epsilon}(t), \tag{7}$$

where $\mathbf{a}_M$ is the acceleration sensor reading which is a noisy measurement of gravitation in the smartphone coordinate system, and $\mathbf{g}_W = \begin{pmatrix} 0 & 0 & g \end{pmatrix}^T$ with $g \approx 9.81\,\text{m/s}^2$ is the global gravitation. We are now interested in the rotation quaternion defining the orientation of the device. For that we need to have an equation for the time-behavior of the quaternion.

The time-dependence of the quaternion can be expressed as a differential equation driven by the local angular velocity (e.g. [6], [11])

$$\frac{d\mathbf{q}(t)}{dt} = \frac{1}{2}\,\mathbf{q}(t)\,\boldsymbol{\omega}_L(t). \tag{8}$$

Because the gyroscope measurement $\boldsymbol{\omega}_M(t)$ is only a noisy version of $\boldsymbol{\omega}_L(t)$, as function of the gyroscope measurement it is advisable to add a noise process to the equation leading to

$$\frac{d\mathbf{q}(t)}{dt} = \frac{1}{2}\,\mathbf{q}(t)\,\boldsymbol{\omega}_M(t) + \mathbf{w}_q(t). \tag{9}$$

Equations (7) and (9) define a state-space model which is compatible with extended Kalman filters [7], [8] as well as various other non-linear Kalman filters (e.g. [9], [15]–[17])—but there are certain practical problems in this formulation, which we discuss in the next section.

C. Disadvantages of Quaternion Representation

The fundamental problem in the quaternion-based state-space formulation above is that it is not observable. This is because we can always replace the quaternion $\mathbf{q}(t)$ with another quaternion $\mathbf{q}_{\mathbf{g}_W}(t)\,\mathbf{q}(t)$, where $\mathbf{q}_{\mathbf{g}_W}(t)$ represents rotation around the global gravitation $\mathbf{g}_W$. The rotation angle of $\mathbf{q}_{\mathbf{g}_W}(t)$ can be arbitrary without affecting the output of the model and hence the system is not observable. This problem would be automatically solved [11] if we had an independent orientation measurement, for example, based on the magnetic field, but here we assume that it is not available.

Another problem with the quaternion representation is that even if it was observable, the requirement of the quaternion to have a unit length often causes numerical problems in the non-linear Kalman filter. These numerical problems are due to null eigenvalues caused by the forced quaternion normalizations after the process noise and estimation errors distract the length of the quaternion away from unity.

It is, however, possible to derive a stable tracking algorithm for the quaternion representation by reformulating the problem as stochastic gradient descent as is done in Madgwick's algorithm [10]. In that approach the non-observability of the model does not matter, because the non-observable rotation is simply left as arbitrary. However, this is not (directly) possible in non-linear Kalman filter kind of approaches, because the covariance of the unobservable subspace grows without a bound which causes the filter to eventually diverge. Although it is possible to fix this problem by introducing pseudo-measurements, we take another route of getting rid of the quaternions altogether.

D. Quaternion-Free Representation

The quaternion-free representation can be derived by deriving a differential equation directly for the gravitation in the local coordinates (cf. [11] page 48). The equation for the local gravitation is given as

$$\mathbf{g}_L(t) = \mathbf{q}^*(t)\,\mathbf{g}_W\,\mathbf{q}(t). \tag{10}$$

Because the global gravitation is constant, by differentiating both sides and using (8) we get

$$\begin{aligned}
\frac{d}{dt}\mathbf{g}_L(t) &= \frac{d}{dt}\left[\mathbf{q}^*(t)\,\mathbf{g}_W\,\mathbf{q}(t)\right] \\
&= \left(\frac{d\mathbf{q}^*(t)}{dt}\right)\mathbf{g}_W\,\mathbf{q}(t) + \mathbf{q}^*(t)\,\mathbf{g}_W\left(\frac{d\mathbf{q}(t)}{dt}\right) \\
&= \left(-\frac{1}{2}\,\boldsymbol{\omega}_L(t)\,\mathbf{q}^*(t)\right)\mathbf{g}_W\,\mathbf{q}(t) \\
&\quad + \mathbf{q}^*(t)\,\mathbf{g}_W\left(\frac{1}{2}\,\mathbf{q}(t)\,\boldsymbol{\omega}_L(t)\right) \\
&= -\frac{1}{2}\,\boldsymbol{\omega}_L(t)\,\mathbf{g}_L + \frac{1}{2}\,\mathbf{g}_L\,\boldsymbol{\omega}_L(t) \\
&= -\boldsymbol{\omega}_L(t) \times \mathbf{g}_L.
\end{aligned} \tag{11}$$

If we further put an additional noise process into the differential equation above while we replace $\boldsymbol{\omega}_L$ with its noisy gyroscope version $\boldsymbol{\omega}_M$ we get the following quaternion-free equations

$$\begin{aligned}
\frac{d\mathbf{g}_L(t)}{dt} &= -\boldsymbol{\omega}_M(t) \times \mathbf{g}_L(t) + \mathbf{w}_g(t), \\
\mathbf{a}_M(t) &= \mathbf{g}_L(t) + \boldsymbol{\epsilon}(t).
\end{aligned} \tag{12}$$

where $\mathbf{w}_g(t)$ is a white noise process. These equations contain the local gravitation direction as the state instead of the orientation quaternions and therefore they are completely linear in the state. Because the full quaternion no longer enters the state, the previous rotation ambiguity is eliminated and the above system is fully observable.

III. ADAPTIVE KALMAN FILTER AND SMOOTHER

A. Kalman Filter For Accelerations and Gyroscopes

To find the connection to state-space modeling and Kalman filtering [8], [9], [15], let us introduce the following notation. Note that in practice, we get measurements from the acceleration sensors at certain discrete instants of time $t_1, t_2, t_3, \ldots$. We assume that we are actually getting point-measurements of the accelerations, plus some noise. For the purposes of modeling, we also assume that the gyroscope signals are piece-wise constant on the intervals $[t_{k-1}, t_k]$ (called zeroth-order-hold, ZOH)—which is an assumption that can be relaxed later, but should work fine with moderately high sampling frequencies. We will write

$$
\begin{aligned}
\mathbf{x}(t) &\triangleq \mathbf{g}_L(t), \\
\mathbf{F}_k &\triangleq -[\boldsymbol{\omega}_M(t_k)]_\times, \\
\mathbf{y}_k &\triangleq \mathbf{a}_M(t_k).
\end{aligned}
\tag{13}
$$

where $[\boldsymbol{\omega}]_\times$ denotes the cross product matrix such that $[\boldsymbol{\omega}]_\times \mathbf{v} = \boldsymbol{\omega} \times \mathbf{v}$. We now model the noise process $\mathbf{w}_g(t)$ as a Gaussian white noise with a spectral density $\mathbf{Q}_c = q_c \, \mathbf{I}$ and the measurement noise as a white Gaussian noise sequence $\boldsymbol{\varepsilon}_k \sim N(0, \sigma^2 \, \mathbf{I})$. Hence our model takes the form

$$
\begin{aligned}
\frac{d\mathbf{x}}{dt} &= \mathbf{F}_k \, \mathbf{x} + \mathbf{w}, \\
\mathbf{y}_k &= \mathbf{x}(t_k) + \boldsymbol{\varepsilon}_k,
\end{aligned}
\tag{14}
$$

which is a special case of a continuous-discrete Kalman filtering problem [15]. We can now convert this model into an equivalent discrete-time (Kalman filtering) model (see, e.g., [15]) as

$$
\begin{aligned}
\mathbf{x}_k &= \mathbf{A}_k \, \mathbf{x}_{k-1} + \mathbf{q}_{k-1}, \\
\mathbf{y}_k &= \mathbf{x}_k + \boldsymbol{\varepsilon}_k,
\end{aligned}
\tag{15}
$$

where $\mathbf{q}_{k-1} \sim N(0, \mathbf{Q}_k)$ and

$$
\begin{aligned}
\Delta t_k &= t_k - t_{k-1}, \\
\mathbf{A}_k &= e^{\mathbf{F}_k \, \Delta t_k}, \\
\mathbf{Q}_k &= \int_{t_{k-1}}^{t_k} e^{\mathbf{F}_k \, (t_k - s)} \, \mathbf{Q}_c \left(e^{\mathbf{F}_k \, (t_k - s)} \right)^T ds.
\end{aligned}
\tag{16}
$$

Using the Rodrigues' rotation formula and recalling that rotation matrices satisfy $\mathbf{C} \, \mathbf{C}^T = \mathbf{I}$, we now get the following explicit expressions:

$$
\begin{aligned}
\mathbf{A}_k &= e^{-[\boldsymbol{\omega}_L(t_k) \, \Delta t_k]_\times} \\
&= \mathbf{I} + \sin(\theta_k) \frac{[-\boldsymbol{\omega}_L(t_k)]_\times}{|\boldsymbol{\omega}_L(t_k)|} + (1 - \cos(\theta_k)) \frac{[-\boldsymbol{\omega}_L(t_k)]_\times^2}{|\boldsymbol{\omega}_L(t_k)|^2}, \\
\mathbf{Q}_k &= q_c \int_{t_{k-1}}^{t_k} e^{-[\boldsymbol{\omega}_L(t_k) \, (t_k - s)]_\times} \left(e^{-[\boldsymbol{\omega}_L(t_k) \, (t_k - s)]_\times} \right)^T ds \\
&= q_c \, \Delta t_k \, \mathbf{I},
\end{aligned}
\tag{17}
$$

where $\theta_k = |\boldsymbol{\omega}_L(t_k)| \, \Delta t_k$. Thus we can estimate the local gravitation vectors $\mathbf{g}_L(t_k) \triangleq \mathbf{x}_k$ by running a Kalman filter and possibly a smoother to the model (15) with the matrices defined in (17).

B. Adaptive Gating of High Accelerations

The state-space formulation in the previous sections is based on the assumption that the accelerometers measure the gravitation plus possibly some small noise. In practice, however, the accelerations of the device can be quite high compared to gravitation. What happens is that when high accelerations are present, the gravitation direction changes a bit towards the external acceleration. Thus the device seems to "lean" towards the acceleration when moved rapidly.

One way to diminish the effect above is to assume that the measurement noise of the model is much higher when there are other accelerations affecting the measurements. What happens is that during periods of high external accelerations, we trust gyro much more (or even completely). The problem then reduces to determining the periods of high acceleration and deciding on a stable logic for increasing the measurement noise.

In the mechanism used here we base the logic onto the following principles:

1) The high accelerations occur as "peaks" which correspond to a Gaussian noise with high variances.
2) Given that there have been no peaks recently, a single peak occurs according to a Poisson process with a certain mean/variance parameter (which is implicit here).
3) Given that there was a single peak, subsequent peaks are likely to occur with a probability which vanishes exponentially in time.

The above assumptions can be approximately mechanized with the following principles.

1) We assume that the measurement noise has the form

$$
\Sigma = (\sigma^2 + \alpha(t)) \, \mathbf{I}, \tag{18}
$$

where σ^2 is a fixed base-level noise and $\alpha(t) \geq 0$ is the peak related part.

2) At each measurement, we do a test whether

$$
\boldsymbol{\nu}_k^T \, \mathbf{S}_k^{-1} \, \boldsymbol{\nu}_k > \gamma, \tag{19}
$$

where $\boldsymbol{\nu}_k$ is the innovation, $\mathbf{S}_k$ is the innovation covariance and γ is a fixed parameter (we use $\gamma = 4$). This is actually a statistical test to determine if the measurement was an outlier, that is, a peak.

3) If it happens that the above test is positive, we set

$$
\alpha(t_k) \leftarrow \alpha_+, \tag{20}
$$

where α_+ is some fixed value (e.g., 10^2).

4) The time-behavior of $\alpha(t)$ is assumed to follow the differential equation

$$
\frac{d\alpha(t)}{dt} = -(1/\tau) \, \alpha(t), \tag{21}
$$

where τ is a relaxation constant (e.g., $1/2$).

Input: Static parameters σ^2, q_c, α_+, γ, τ, α_0, $\mathbf{m}_0$, $\mathbf{P}_0$; times and measurements $t_k, \mathbf{y}_k$, $k = 1, \ldots, n$.
Output: Filter means and covariances $\mathbf{m}_k, \mathbf{P}_k$ and model matrices $\mathbf{A}_k, \mathbf{Q}_k$ for $k = 1, \ldots, n$.

1: **for** $k = 1, \ldots, n$ **do**
2:     Compute $\mathbf{A}_k$ and $\mathbf{Q}_k$ via (17).

3:     $\mathbf{m}_k^- \leftarrow \mathbf{A}_k \mathbf{m}_{k-1}$ ▷ Kalman filter prediction
4:     $\mathbf{P}_k^- \leftarrow \mathbf{A}_k \mathbf{P}_{k-1} \mathbf{A}_k^T + \mathbf{Q}_k$

5:     $\alpha_k \leftarrow \exp(-\Delta t_k/\tau)\,\alpha_{k-1}$ ▷ Noise relaxation

6:     $\boldsymbol{\nu}_k \leftarrow \mathbf{y}_k - \mathbf{m}_k^-$ ▷ Innovation mean and covariance
7:     $\Sigma_k \leftarrow (\sigma^2 + \alpha_k)\,\mathbf{I}$
8:     $\mathbf{S}_k \leftarrow \mathbf{P}_k^- + \Sigma_k$

9:     **if** $\boldsymbol{\nu}_k^T \mathbf{S}_k^{-1} \boldsymbol{\nu}_k > \gamma$ **then**   ▷ Outlier detection
10:         $\alpha_k \leftarrow \alpha_+$ ▷ Increased noise
11:         $\Sigma_k \leftarrow (\sigma^2 + \alpha_k)\,\mathbf{I}$
12:         $\mathbf{S}_k \leftarrow \mathbf{P}_k^- + \Sigma_k$ ▷ New innovation covariance
13:     **end if**

14:     $\mathbf{K}_k \leftarrow \mathbf{P}_k^- \mathbf{S}_k^{-1}$ ▷ Kalman filter update
15:     $\mathbf{m}_k \leftarrow \mathbf{m}_k^- + \mathbf{K}_k \boldsymbol{\nu}_k$
16:     $\mathbf{P}_k \leftarrow \mathbf{P}_k^- - \mathbf{K}_k \mathbf{S}_k \mathbf{K}_k^T$
17: **end for**

Fig. 2.   Pseudo-code for the adaptive Kalman filter (AKF) algorithm. Note that a non-adaptive Kalman filter (KF) can be obtained by setting $\alpha_0 = 0$ and $\gamma = \infty$.
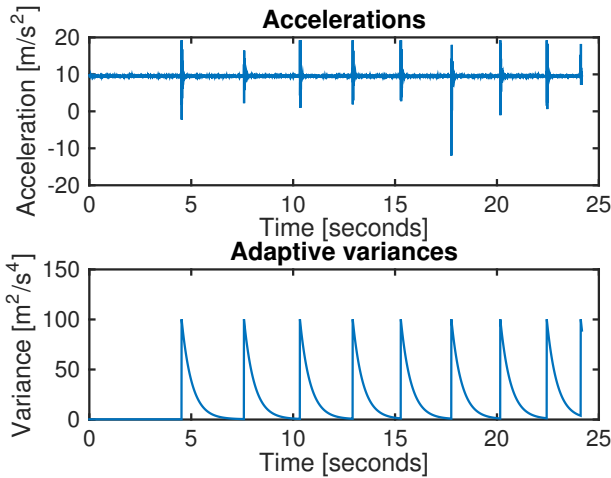

Fig. 3.   Simple test of the effect of tapping the smartphone to the variance adaptation. Each tap causes a noise peak which then triggers the adaptation which increases the noise level. The noise returns to the original level exponentially.

The resulting adaptive filtering algorithm is shown in Fig. 2. Fig. 3 illustrates the operation of the adaptation algorithm in a scenario, where we tapped the smartphone screen such that it causes a significant acceleration peak.

Input: Filter means and covariances $\mathbf{m}_k, \mathbf{P}_k$ and model matrices $\mathbf{A}_k, \mathbf{Q}_k$ for $k = 1, \ldots, n$.
Output: Smoother means and covariances $\mathbf{m}_k^s, \mathbf{P}_k^s$ for $k = 1, \ldots, n$.

1: $\mathbf{m}_n^s \leftarrow \mathbf{m}_n$ ▷ Initialize
2: $\mathbf{P}_n^s \leftarrow \mathbf{P}_n$

3: **for** $k = n - 1, \ldots, 1$ **do**
4:     $\mathbf{m}_{k+1}^- \leftarrow \mathbf{A}_{k+1} \mathbf{m}_k$ ▷ RTS smoother recursion
5:     $\mathbf{P}_{k+1}^- \leftarrow \mathbf{A}_{k+1} \mathbf{P}_k \mathbf{A}_{k+1}^T + \mathbf{Q}_{k+1}$
6:     $\mathbf{G}_k \leftarrow \mathbf{P}_k \mathbf{A}_{k+1}^T [\mathbf{P}_{k+1}^-]^{-1}$
7:     $\mathbf{m}_k^s \leftarrow \mathbf{m}_k + \mathbf{G}_k [\mathbf{m}_{k+1}^s - \mathbf{m}_{k+1}^-]$
8:     $\mathbf{P}_k^s \leftarrow \mathbf{P}_k + \mathbf{G}_k [\mathbf{P}_{k+1}^s - \mathbf{P}_{k+1}^-] \mathbf{G}_k^T$
9: **end for**

Fig. 4.   Pseudo-code for the Kalman smoother (both KS and AKS) algorithm.

C. Kalman Smoother

The adaptive Kalman filter algorithm introduced above has the property that it only uses measurements up to current time step for forming its estimate. This is indeed the only possibility in real-time operation, but sometimes it is possible to collect some data and then do the estimation using all the data. The algorithms for conditioning the estimate on all the data retrospectively are often called smoothing algorithms (see, e.g., [9]). It is expected that conditioning on all the data with a smoother leads to a better estimate than what the filter produces.

A simple implementation of a smoothing algorithm is shown in Fig. 4. The smoother is actually a Rauch–Tung–Striebel (RTS) type of linear smoother which has the property that the smoothing solution is independent of the measurement noise covariances and hence in that sense independent of the adaptation mechanism. Therefore the smoothing algorithm is identical to a smoother for the case of no adaptation at all. However, strictly speaking, the smoothing algorithm is not optimal for the case with adaptation, because we should actually condition the noise adaptation on the whole data as well, whereas now it only uses the previous measurements in the same way as the filter does. However, the approximate smoother can still be expected to improve the filter estimates.

It would also be possible to replace the full smoothing recursion with the fixed-lag smoother (see, e.g., [9]) which uses only small horizon of future measurements to form its estimate. The disadvantage is that this introduces a delay to the estimates. However, if such a delay is tolerated, fixed-lag smoothing can provide almost as good estimates as the full smoothing solution in almost real time.

IV. EXTENSIONS AND DISCUSSION

A. Asyncronous Sensors

Although in the previous section the model was formulated by assuming that the gyroscope and acceleration measurements are obtained at same time instants, it is not actually required. We can well think that for the most steps k, we only have gyroscope measurement—then in the Kalman filter we only do Kalman filter prediction, no update at all. When we

have an acceleration sensor measurement, we should then do Kalman filter prediction exactly to the time when we have the measurement. This can be done by extending the previous gyroscope measurement up to the measurement time and doing Kalman filter prediction for that. On the next prediction step we then need to recall to shorten the time span of the next gyroscope measurement accordingly.

B. Acceleration Sensor Bias Estimation

It would also be possible to estimate the acceleration sensor biases jointly with the gravitation. This can be implemented by introducing an unknown bias vector into the measurement model:

$$\mathbf{a}_M(t) = \mathbf{g}_L(t) + \mathbf{b}(t) + \boldsymbol{\epsilon}(t). \tag{22}$$

We can then augment the bias into the state together with the local gravitation and assume that it has the dynamic model

$$\frac{d\mathbf{b}}{dt} = \mathbf{w}_b(t), \tag{23}$$

where $\mathbf{w}_b(t)$ is a white noise process with a "small" (possibly zero) spectral density. The adaptive Kalman filters and smoothers can be then implemented in an analogous manner to Section III.

C. Low Gyroscope Sampling Rates

When the sampling rates of the sensors are small, the zeroth-order-hold (ZOH) approximation used in the gyroscope measurements can cause problems. Fortunately, it is possible to derive the discretization equations for the first-order-hold (FOH) or even higher order approximations which essentially approximate the continuous gyroscope measurement signal by using linear or polynomial interpolation. However, even simpler approach is to simply oversample the gyroscope measurements using a suitable interpolation method. This approach requires no changes to the algorithms, only an additional resampling step in front of them.

D. Algorithm Stability

One advantage of the present adaptive Kalman filter formulation is that it can easily be proven to be asymptotically stable. The intuition behind this is that if we fix the measurement sequence, the measurement noises always remain uniformly bounded from below and above. Furthermore, because the model is uniformly controllable and observable, the Theorem 7.4 of [7] shows that the filter is asymptotically stable. Because the smoother is just the ordinary RTS smoother, the classical results imply that it is asymptotically stable as well.

It is worth noting that this kind of general stability results are not available for non-linear Kalman filters and generally one cannot ensure stability of such a non-linear filter with any practically sensible parameter values (see, e.g., [18]). However, it is sometimes possible to prove the stability of specific non-linear filters, but this needs to be done for each case separately.
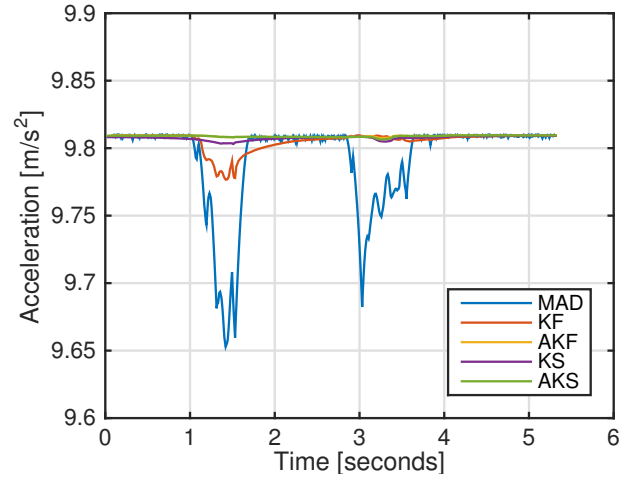

Fig. 5.   Z-component of gravitation in the 90-degree rotation test.

V.   EXPERIMENTAL RESULTS

We tested the proposed algorithms against the Madgwick's algorithm [10], which is a well-known quaternion-based algorithm for tracking the gravitation direction. The tested algorithms are labeled as follows:

- **MAD**: The Madgwick's algorithm.

- **KF**: Kalman filter on the proposed state-space model without adaptive gating.

- **AKF**: Kalman filter on the proposed state-space model with adaptive gating.

- **KS**: Kalman smoother on the proposed state-space model without adaptive gating.

- **AKS**: Kalman smoother on the proposed state-space model with adaptive gating.

A. 90-degree rotation test

In this experiment we first put the device on a table, then we quickly rotated it 90 degrees around z-axis and 90-degrees back. What we should see is that the measured gravitation changes to another value for a while and then returns back to its original value.

The Fig. 5 shows the estimates of the z-components of gravitation for each method. It can be seen that the rotation causes a huge discrepancy to the gravitation estimate for Madgwick (MAD), and a significant discrepancy also for the KF and KS. The adaptive algorithms in turn are able to track the gravitation very well despite the fast turn.

Figs. 6 and 7 show the x- and y-components of the gravitation estimate, which show that some of the gravitation in MAD/KF/KS has "leaked" to these components. In practical terms this means that there is a "leaning" effect in the estimates meaning that the extra accelerations caused by the fast rotation causes the gravitation to slightly turn sideways. This effect is significantly smaller in AKF/AKS than in the other methods.

Fig. 8 shows the adaptive variance of the AKF and AKS methods. Clearly the algorithm has identified the instants of
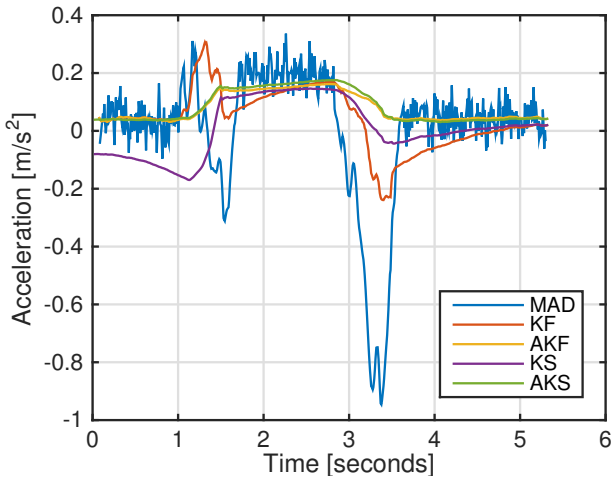
Fig. 6.   Y-component of gravitation in the 90-degree rotation test.
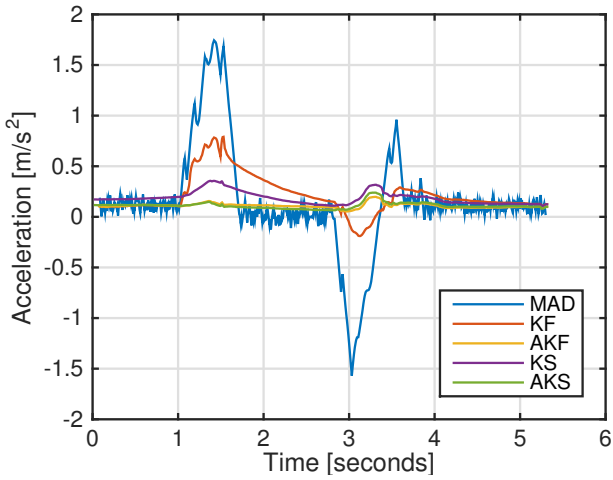

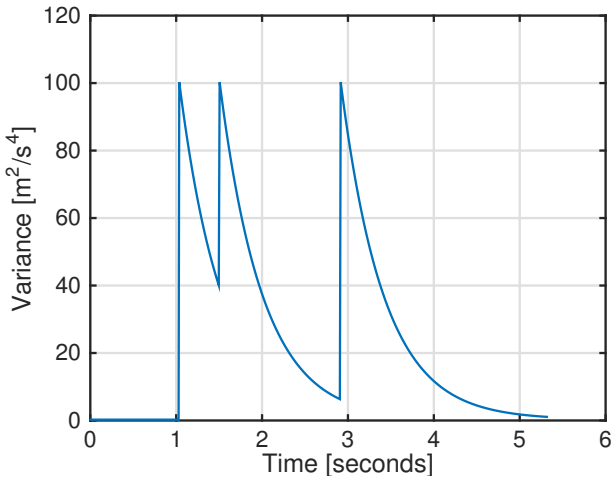Fig. 7.   X-component of gravitation in the 90-degree rotation test.

Fig. 8.   The adaptive noise parameter in the 90-degree rotation test.

the fast accelerations and reduced the effect of acceleration to the estimates for a moment. As can be seen in the gravitation estimates, this reduces the disturbance caused by the fast rotations significantly.
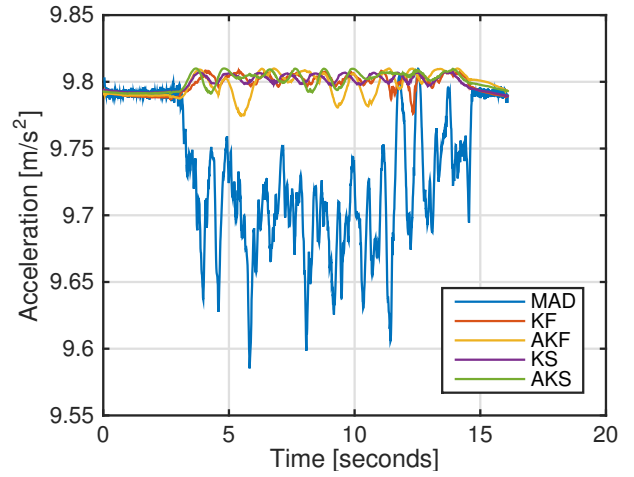

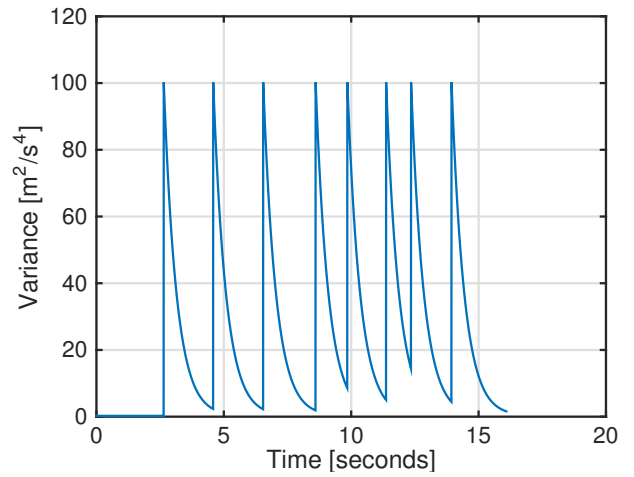Fig. 9.   Z-component of gravitation in the multi-round rotation test.

Fig. 10.   The adaptive noise parameter in the multi-round rotation test.

B. Multi-round rotation test

In this test we installed a smartphone to a balanced platform which we could rotate while keeping the gravitation direction constant. Fig. 9 shows the estimated gravitation direction from each of the algorithms. It can be seen that the Madgwick (MAD) algorithm has significant challenges in keeping up with the gravitation as it has a significant bias. The Kalman filters and smoothers do much better in this case—actually it might be that the non-adaptive algorithms KF/KS do slightly better than the adaptive algorithms AKF/AKS, because in this case the adaptation might not actually be necessary. However, as can be seen in Fig. 10 the rotation still triggers the adaptation.

VI.   CONCLUSION

In this paper we have presented a convenient linear state-space for Kalman and smoother based tracking of gravitation direction in mobile devices such as smartphones. We have also proposed an adaptation mechanism to cope with high accelerations in the Kalman filtering. The experimental results show that the Kalman filters and smoothers have a smaller noise than the compared algorithm and the adaptation reduces the leaning effect caused by accelerations during fast turns.

REFERENCES

[1] Z. Xiao, H. Wen, A. Markham, and N. Trigoni, "Robust pedestrian dead reckoning (R-PDR) for arbitrary mobile device placement," in *International Conference on Indoor Positioning and Indoor Navigation (IPIN)*, vol. 27, 2014.

[2] I. Vallivaara, J. Haverinen, A. Kemppainen, and J. Roning, "Simultaneous localization and mapping using ambient magnetic field," in *IEEE Conference on Multisensor Fusion and Integration for Intelligent Systems (MFI)*, 2010, pp. 14–19.

[3] B. Li, T. Gallagher, A. G. Dempster, and C. Rizos, "How feasible is the use of magnetic field alone for indoor positioning?" in *Proceedings of the International Conference on Indoor Positioning and Indoor Navigation (IPIN)*, Sydney, Australia, November 2012, pp. 1–9.

[4] M. Kok and T. Schön, "Maximum likelihood calibration of a magnetometer using inertial sensors," in *Proceedings of the 19th IFAC World Congress*, 2014, pp. 92–97.

[5] M. S. Grewal, L. R. Weill, and A. P. Andrews, *Global Positioning Systems, Inertial Navigation and Integration*. Wiley, 2001.

[6] D. H. Titterton and J. L. Weston, *Strapdown Inertial Navigation Technology*. The Institution of Electrical Engineers, 2004.

[7] A. H. Jazwinski, *Stochastic Processes and Filtering Theory*. Academic Press, New York, 1970.

[8] M. S. Grewal and A. P. Andrews, *Kalman Filtering, Theory and Practice Using MATLAB*. Wiley, 2001.

[9] S. Särkkä, *Bayesian filtering and smoothing*. Cambridge University Press, 2013.

[10] S. O. Madgwick, A. J. Harrison, and R. Vaidyanathan, "Estimation of IMU and MARG orientation using a gradient descent algorithm," in *IEEE International Conference on Rehabilitation Robotics (ICORR)*, 2011, pp. 1–7.

[11] J. Hol, "Sensor fusion and calibration of inertial sensors, vision, ultra-wideband and GPS," Linköping Studies in Science and Technology. Dissertations. No. 1368, Linköping University, The Institute of Technology, Jun 2011.

[12] J.-O. Nilsson, A. K. Gupta, and P. Händel, "Foot-mounted inertial navigation made easy," in *2014 International Conference on Indoor Positioning and Indoor Navigation (IPIN)*, 2014.

[13] S. Särkkä and A. Nummenmaa, "Recursive noise adaptive Kalman filtering by variational Bayesian approximations," *IEEE Transactions on Automatic Control*, vol. 54, no. 3, pp. 596–600, 2009.

[14] R. Piché, S. Särkkä, and J. Hartikainen, "Recursive outlier-robust filtering and smoothing for nonlinear systems using the multivariate Student-t distribution," in *Proceedings of IEEE International Workshop on Machine Learning for Signal Processing (MLSP)*, 2012.

[15] S. Särkkä, "Recursive Bayesian inference on stochastic differential equations," Doctoral dissertation, Helsinki University of Technology, 2006.

[16] ——, "On unscented Kalman filtering for state estimation of continuous-time nonlinear systems," *IEEE Transactions on Automatic Control*, vol. 52, no. 9, pp. 1631–1641, 2007.

[17] S. Särkkä and J. Sarmavuori, "Gaussian filtering and smoothing for continuous-discrete dynamic systems," *Signal Processing*, vol. 93, no. 2, pp. 500–510, 2013.

[18] K. Reif, S. Günther, E. Yaz, and R. Unbehauen, "Stochastic stability of the discrete-time extended Kalman filter," *IEEE Transactions on Automatic Control*, vol. 44, no. 4, pp. 714–728, 1999.